

# Influence of ion bombardment flux on the characteristics of NiC films obtained by cathodic arc deposition

M. BALACEANU, A. VLADSCU, M. BRAIC\*, C. N. ZOITA, I. FERARU, V. BRAIC  
National Institute for Optoelectronics, P.O.Box MG-5, RO 077125, Bucharest, Romania

This paper aims to provide an analysis on the effects of ion bombardment flux ( $j_i$ ) on film characteristics of nickel carbide films deposited by the cathodic arc method, under the conditions when ion energy ( $E_i$ ) and the ratio of the ion flux to the flux of deposited atoms ( $j_i/j_a$ ) were kept constant. The deposition atmosphere consisted in a  $\text{CH}_4+\text{Ar}$  mixture. The substrate current density was varied from 2.7 to 4.4  $\text{mA}/\text{cm}^2$  by using either one or two cathodes. The coatings were investigated in terms of elemental and phase composition, texture, chemical bondings, residual stress, hardness, electrical characteristics and tribological performance. The experimental results showed that film crystallinity, hardness and wear resistance of the NiC coatings improved at increased ion bombardment intensity.

(Received November 26, 2010; accepted November 29, 2010)

*Keywords:* Nickel carbide, Cathodic arc, Mechanical properties, Electrical resistivity

## 1. Introduction

It has been known for many years that the ion bombardment during thin films growth induces changes in chemical bonds, crystalline orientation, lattice parameter, packing density, intrinsic stress, grain size and surface topography [1– 7].

For a constant substrate temperature, the main parameters characterizing the effects of the ion irradiation are the ion energy  $E_i$ , the ion flux  $j_i$  and deposited atoms flux  $j_a$ . Different authors considered the role played by each parameter and their relative importance in different ways. Thus, in several works the average energy  $E$  delivered per atom ( $E = E_i (j_i/j_a)$ ) was treated as being a performance parameter which correlated bombardment conditions with coating properties [8], [9], while in other works the parameters  $E_i$  and  $j_i/j_a$  were distinctly taken into account since they were considered to influence the film properties through quite different mechanisms [2], [10]. Furthermore, some authors showed that the film properties (microstructure, morphology, intrinsic stress, hardness) depend not only on the ion/neutral flux ratio, but also on the absolute value of the ion current density [1], [4], [10]. It has been also reported that the major role in improving coating quality (in terms of coating densification) is played by the coating sputtering, in which the relative importance of ion energy and flux depends on the energy range [1].

This paper focuses on the effects of ion flux  $j_i$  on the properties of nickel carbide coatings, obtained at constant  $E_i$  and  $j_i/j_a$  ratio. Film characteristics were analyzed as function of substrate current density  $j_s$  and deposition rate  $D_R$  since these process parameters are, as it is usually admitted, proportional to  $j_i$  and  $j_a$ , respectively. The selection of Ni-C films was determined by the following reasons. Metals with low reactivity to carbon (e.g. Ni) form nanocomposite structures, with the metal or carbide nanocrystals embedded in an amorphous carbon matrix.

Such fine nanocrystalline structures are commonly associated with high hardness and toughness, and good tribological performance. Of these materials, carbon-nickel composite films have been shown to exhibit interesting mechanical, tribological and electrical properties (low level of residual stress, good friction behavior, significant change of resistivity with carbon content variation) [11 – 14].

The coatings were deposited by the cathodic arc method on C45 steel and Si substrates. The films were analyzed for elemental and phase composition, texture, mechanical characteristics (residual stress and hardness), electrical resistivity and tribological behavior.

## 2. Experimental

The coatings were prepared in a cathodic arc unit [15] equipped with two Ni cathodes. The reactive atmosphere was a mixture of Ar and  $\text{CH}_4$  gases. Two coating types were prepared, having different substrate current densities  $j_s$  and deposition rates  $D_R$ , but the same  $j_s/D_R$  ratio and substrate bias voltage  $V_s$ . The change of the substrate current density, and also of the deposition rate, was obtained by using either one cathode (sample NiC-1, Table 1) or two cathodes (sample NiC-2, Table 1). To have a constant  $j_s/D_R$  value for both samples, the cathode currents were accordingly adjusted (see Table 1). The substrates were not intentionally heated, their temperature being around  $100^\circ\text{C}$ . Furthermore, in order to keep constant the elemental compositions of the films when employing one or two cathodes, the mass flow rate of the reactive gas ( $\text{CH}_4$ ) was properly controlled. For all coatings' deposition, the argon flow rate and the substrate bias were held constant at 30 sccm and -100 V, respectively, while the cathode currents were as listed in Table 1, in which the measured  $j_s$  and  $D_R$  values, as well as the  $j_s/D_R$  ratio, are also given.

Table 1. Deposition conditions for InN films.

Sample	Number of cathodes	$I_c$ (A)		$F_R$ (sccm)	$j_s$ (mA/cm <sup>2</sup> )	$D_R$ (nm/s)	$j_s/D_R$ ( $\frac{mA \cdot s}{cm^2 \cdot nm}$ )
		Cathode 1	Cathode 2				
NiC-1	1	110	-	120	2.7	1.3	2.08
NiC-2	2	115	115	200	4.4	2.1	2.10

Under these deposition conditions, the  $j_s/D_R$  ratio was of approximately 2.1 mA·s/cm<sup>2</sup>·nm for all coatings.

Deposition periods were selected to prepare films of approximately 2.4 μm thick.

Depth profiles of atomic concentrations were obtained by GDOS analysis, using a SPECTRUMA GDA-750 HP spectrometer. The carbon binding state in the films was investigated by Raman spectroscopy. The spectra were taken with a LABRAM-HT spectrometer, using the 488 nm excitation wavelength of a HeNe laser. Phase composition and preferred orientations were studied by X-ray diffraction (Rigaku MiniFlex II, Cu K<sub>α</sub> radiation).

The film thickness and residual stress were determined with a Dektak 150 surface profiler. For residual stress determination, radius of curvature of silicon substrates (2 inches in diameter) was measured prior and after film deposition. Film hardness was measured with a FM-700 Digital Microhardness Tester (0.1 N load). The films' resistivity was determined by the Van der Pauw method using the HMS-3000 Hall Effect Measurement System. Tribological performance of coatings was examined in dry atmosphere by means of a CSEM Ball-on-Disc Tribometer (sapphire ball of 6 mm in diameter, 0.2 m/s, 400 m sliding distance, 3 N load).

### 3. Results and discussion

#### 3.1. Elemental composition, crystalline structure and chemical bondings

The chemical composition depth profiles of the NiC coatings deposited on C45 steel substrates were obtained by GDOS technique. Table 2 displays the atomic percentages of Ni, C and O determined at a depth of about 1 μm (equilibrium values) and considered to represent the values in the film bulk.

As an example, the chemical composition depth profile of a NiC coating (sample NiC-1) deposited on a C45 steel substrate, as obtained by GDOS, is shown in Fig. 1. It should be noted that both films are almost stoichiometric, having similar atomic concentrations (C/Ni = 0.93 - 0.96).

The phase composition, texture and crystalline structure of the nickel carbide films were analyzed by X-ray diffraction. The diffraction patterns (Fig. 2) show the presence of two phases in the deposited films: Ni<sub>3</sub>C (hexagonal closed-packaged hcp, (113) texture) and NiC (fcc, (111) texture). The enhancement of the ion flux determines more intense peaks, indicating an improvement of film crystallinity and an increase in crystallite size  $d$ , as presented in Table 3.

Table 2. Elemental composition of the NiC coatings

Sample	Elemental composition (at.%)			C/Ni
	Ni	C	O	
NiC-1	50.8	47.1	2.1	0.93
NiC-2	50.3	48.3	1.4	0.96

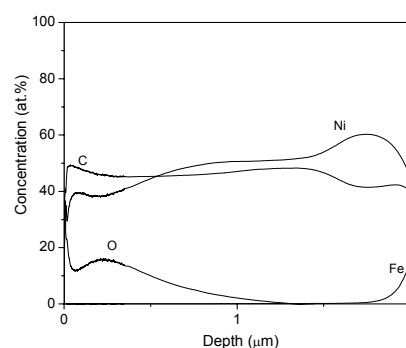


Fig. 1. GDOS depth profiles of a NiC coating (sample NiC-1).

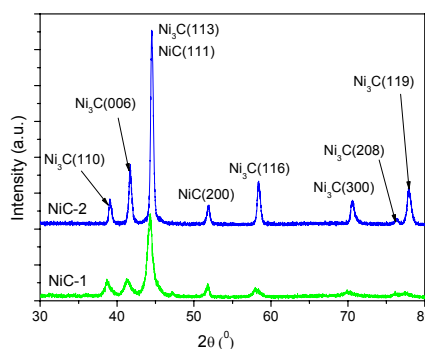


Fig. 2. X-ray diffraction patterns of the NiC coatings.

The carbon bondings in the films were investigated by Raman spectroscopy (Fig. 3). The Raman spectra are typical for metal containing carbon films. The appearance of bands D and G is indicative of the presence of C-C bonds. This result, correlated with those obtained by X-ray diffraction, shows that the films have a composite structure: crystalline Ni<sub>3</sub>C and NiC phases, embedded in an amorphous carbon (a-C) matrix.

In Table 3, the G peak position and  $I_D/I_G$  ratios in the deposited films are presented. It can be seen that G peak position shifts towards higher wavenumbers and the  $I_D/I_G$  ratio increase with the ion flux enhancement, indicating an increase in the clustering of the ring - like sp<sup>2</sup> structure of the metal - free carbon phase [16], [17].

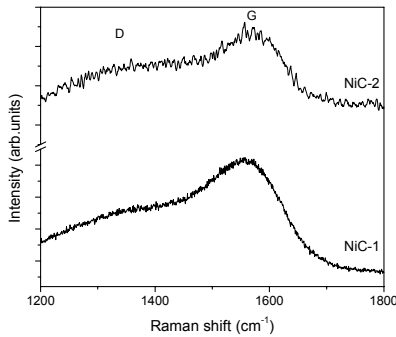


Fig. 3. Raman spectra of the NiC coatings.

Table 3. G peak position and  $I_D/I_G$  ratio in the NiC films.

Sample	G Position (cm <sup>-1</sup> )	$I_D/I_G$
NiC-1	1551	1.02
NiC-2	1562	1.15

### 3.2. Mechanical characteristics

The measured values of residual stress and hardness of the nickel carbide coatings are summarized in Table 4. It can be seen that the variation of the substrate current density induces changes in residual stress. The films grown under reduced ion bombardment exhibit a compressive stress, which changes into a tensile, as the current density increases. It is known that PVD deposited films develop an intrinsic stress, as the result of non-equilibrium growth conditions. As the investigated films were deposited at relatively low temperature, under the low ion density growth conditions, very little surface diffusion and a large vacancy concentration are expected.

We observed the increase in the grain size for enhanced ion flux, especially for the NiC phase. As the grain boundaries are less dense than the grain lattice, the elimination of lots of grain boundaries leads to a densification of the film and to a change in the developed stress, from compressive to tensile [18, 19], according to the observed increase of the tensile strain in NiC-2 films. However, because the difference in the stress values obtained for the two films is high, we looked also for other explanation, compatible with the first one. We considered that the excess vacancies in the films are partially annihilated due to ion bombardment enhancement. The vacancy annihilation at a vertical boundary results in an in-plane change of film dimensions, so that additional tensile stress develops. We mention that the equally probable vacancy annihilation on the film surface or at the interface add no additional stress since the in-plane dimensions of the film are not changed [20, 21].

The experimental results show an increase in films' hardness with increasing ion bombardment intensity, accompanied by a transition from compressive to tensile

stress and an increase in the mean crystallite size. So, the hardening effect seems to be related neither to the stress developed in the film, nor to Hall-Petch mechanism ( $H \sim (1/d)^{1/2}$ ). Also, the observed hardness increase can not be related to defect hardening, as this is effective only in films under high compressive stress. The beneficial effects of ion bombardment intensity on film hardness could be related to coating densification, due to material redistribution caused by a more intense ion bombardment, as the relative importance of ion energy and flux depends on the energy range [1]. According to Petrov et al. [22], at energies nearby 100 eV, as in our deposition conditions, the film densification is determined by collisional cascade effects such as forward sputtering, recoil implantation and atom mixing. To prove this in our case, we discuss in the following the film's electric resistivity behaviour and the tribological properties.

Table 4. Residual stress ( $\sigma$ ), hardness ( $H$ ), electrical resistivity ( $\rho$ ) and crystallite size ( $d$ ) of the NiC coatings.

Sample	$\sigma$ (MPa)	$H$ (GPa)	$\rho$ ( $\times 10^{-6}$ $\Omega\text{cm}$ )	$d$ (nm) NiC(200)	$d$ (nm) Ni <sub>3</sub> C(006)
NiC-1	-1469	19.5	246	7.8	18.5
NiC-2	+197	25.1	50	21.4	21.8

### 3.3. Electrical resistivity

The results of the resistivity measurements using the four-point probe technique are listed in Table 4.

Depending on the Ni content, NiC coatings present either dielectric or conductive characteristics, the later one for nickel concentrations above  $\sim 21$  at.% [23]. As expected, with a Ni content of about 50 at.%, the deposited coatings exhibited a low electrical resistivity, which depends on the intensity of ion bombardment. If we consider the values of the electrical resistivity as an indication of the internal defects [24], it clearly results the decrease of defect amounts as the current density of ions striking the substrate is increased. The observed reduced resistivity could also be ascribed to the reduced carriers scattering on grain boundaries, according to the X-ray diffraction patterns displaying the grain size increase with the ion flux.

### 3.4. Friction and wear performance

The tribological tests were performed on coatings deposited on C45 steel discs (30 mm in diameter). The results of the tests were summarized in terms of the variation of the friction coefficient  $\mu$  vs. sliding distance (Fig. 4) and of the wear rate  $K$  and friction coefficient after the sliding test (Fig. 5).

One may observe that both the friction coefficient and the wear rate decreased with increasing ion flux, attesting the beneficial effects of ion bombardment intensity on nickel carbide coating characteristics.

Fig. 6 show 3-D images of wear tracks at the end of the friction tests for the samples NiC-1 and NiC-2. It can be seen a less material removal for the coating prepared under enhanced ion flux conditions (sample NiC-2), confirming the above mentioned results.

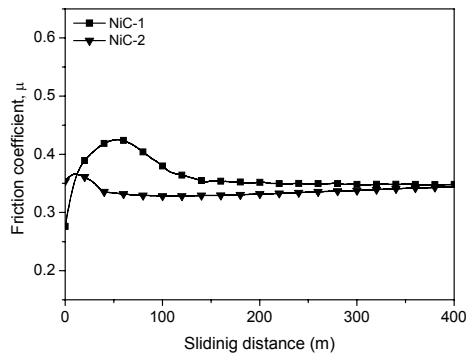


Fig. 4. Friction coefficient  $\mu$  for NiC coatings as a function of sliding distance.

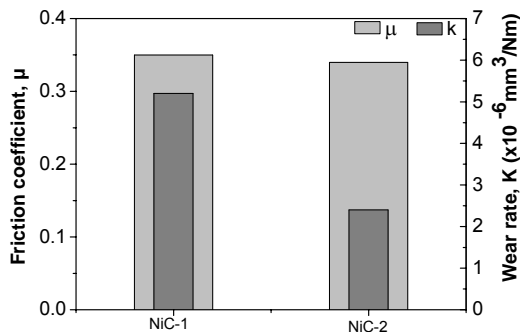


Fig. 5. Friction coefficient  $\mu$  and wear rate  $K$  for NiC coatings (dry testing conditions; sapphire ball, 0.2 m/s, sliding distance 400 m, 3 N load).

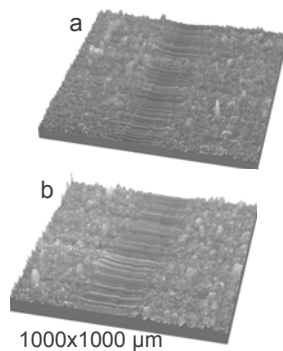


Fig. 6. Two 3-D images of surface profiles of wear tracks for (a) – NiC-1 and (b) – NiC-2 coatings after the sliding test of 400 m.

#### 4. Summary and conclusions

Research carried out demonstrated that the flux of the ions striking the substrate, as determined by the substrate current density  $j_s$ , has a direct influence on the properties of the nickel carbide coatings, distinctly from the ratio  $j_s/D_R$  of the ion flux to the overall flux of deposited particles. The ion flux variation was obtained by using either one or two cathodes, while keeping constant the substrate bias and  $j_s/D_R$  values. Different film characteristics have been observed to depend on the ion flux as follows.

- The coatings, with C/N ratios of about 0.94, exhibit a composite structure, consisting of a mixture of crystalline hcp  $Ni_3C$  and fcc NiC phases, embedded in an amorphous a-C phase. The film crystallinity improved with increasing ion flux.
- The films were found to change from compressive to tensile stress, with increasing ion flux. An increase in hardness with ion flux enhancement was also observed.
- The films prepared under enhanced ion bombardment exhibited superior wear resistance.

In conclusion, we could appreciate that in the case of the NiC coatings and for the deposition conditions under consideration in this work, the enhancement of the ion flux improves the film quality.

#### Acknowledgements

The work was supported under the ERA-NET Project no. MNT 7026/2010.

#### References

- [1] K. S. Fancey, C. A. Porter, A. Matthews, *J. Vac. Technol., A*, **13**, 428 (1995).
- [2] I. Petrov, F. Adibi, J. E. Greene, L. Hultman, J. E. Sundgren, *Appl. Phys. Lett.* **63**, 36 (1993).
- [3] B. Rauschenbach, J. W. Gerlach, *Cryst. Res. Technol.*, **35**, 675 (2000).
- [4] M. M. M. Bilek, D. R. McKenzie, R. N. Tarrant, S. H. N. Lin, D. G. McCulloch, *Surf. Coat. Technol.*, **156**, 136 (2002).
- [5] J. H. Hsieh, C. Li, W. Wu, R. F. Hochman, *Thin Solid Films*, **424**, 103 (2003).
- [6] G. Abadias, Y. Y. Tse, Ph. Guérin, V. Pelosin, *J. Appl. Phys.*, **99**, 113519 (2006).
- [7] J. Musil, J. Šuna, *Mater. Sci. Forum*, **502**, 291 (2005).
- [8] C. A. Davis, *Thin Solid Films*, **226**, 30 (1993).
- [9] S. M. Rossnagel, J. J. Cuomo, *Thin Solid Films*, **171**, 143 (1989).
- [10] H. Windischmann, *Crit. Rev. Solid State Mater. Sci.*, **17**, 547 (1992).
- [11] S. Kukielka, W. Gulbiński, Y. Pauleau, S. N. Dub, J. J. Grob, *Surf. Coat. Technol.*, **200**, 6258 (2006).
- [12] A. Sylvestre, S. Kukielka, D. M. Nguyen, W. Gulbiński, Y. Pauleau, *Rev. Adv. Mater. Sci.* **15**,

- 185 (2007).
- [13] G. Abrasonis, M. Krause, A. Mücklich, K. Sedláčková, G. Radnóczy, U. Kreissig, A. Kolitsch, W. Möller, *Carbon* **45**, 2995 (2007).
- [14] C. P. Lungu, A. M. Lungu, P. Chiru, A. Tudor, R. Brescia, *Int. J. Surf. Sci. Eng.* **4**, 191 (2010).
- [15] A. Vladescu, A. Kiss, A. Popescu, M. Braic, M. Balaceanu, V. Braic, I. Tudor, C. Logofatu, C. C. Negrila, R. Ripeanu, *J. Nanosci. Nanotechnol.* **8**, 717 (2008).
- [16] A. C. Ferari, J. Robertson, *Phys. Rev. B* **61**, 14095 (2000).
- [17] A. C. Ferari, in: C. Donnet, A. Erdemir (Eds.), *Tribology of Diamond-like Carbon Films*, Springer Science, New York, USA, 2008, 41.
- [18] R. W. Hoffman, *Phys. Thin Films* **34**, 185 (1976).
- [19] L. B. Freund, E. Chason, *J. Appl. Phys.* **89**, 4866 (2001).
- [20] P. Chaudhari, *J. Vac. Sc. Tech.* **9**, 520 (1972).
- [21] P. A. Flinn, D. S. Gardner, W. D. Nix, *IEEE Trans. ED-* **34**, 689 (1987).
- [22] I. Petrov, L. Hultman, J. E. Sundgren, *J. Vac. Sci. Technol. A* **10**, 265 (1992).
- [23] A. Sylvestre, S. Kukielka, D. M. Nguyen, W. Gulbiński, Y. Pauleau, *Rev. Adv. Mater. Sci.* **15**, 185 (2007).
- [24] W-J. Chou, Ge-P. Yu, J-H. Huang, *Surf. Coat. Technol.* **140**, 206 (2001).

---

\*Corresponding author: mariana\_braic@inoe.ro